Transformer Fault Analysis Using Event Oscillography

Casper Labuschagne and Normann Fischer
Schweitzer Engineering Laboratories, Inc.

Presented at the
61st Annual Georgia Tech Protective Relaying Conference
Atlanta, Georgia
May 2–4, 2007

Previously presented at the
60th Annual Conference for Protective Relay Engineers, March 2007

Originally presented at the
33rd Annual Western Protective Relay Conference, October 2006

Transformer Fault Analysis Using Event Oscillography

Casper Labuschagne and Normann Fischer, *Schweitzer Engineering Laboratories, Inc.*

***Abstract*—Transformer differential protection operates on Kirchhoff's well-known law that states, "The sum of currents entering and leaving a point is zero." Although Kirchhoff's law is well understood, the implementation of the law in transformer differential protection involves many practical considerations such as current transformer (CT) polarity, phase-angle correction, zero-sequence removal, and CT grounding. Still, even correctly implemented transformer differential protection misoperates occasionally, resulting from conditions such as CT saturation during heavy through faults.**

Whereas electromechanical and electronic relays provide no or very little fault information, numerical relays provide an abundance of information. However, the analyst must still select the correct fault information from this abundance of information to perform useful fault analysis.

This paper demonstrates how to begin analysis of such events by using real-life oscillographic data and going through a step-by-step analysis of the relay algorithm using a mathematical relay model. Relay engineers can use this paper as a reference for analyzing transformer oscillography in a systematic and logical manner.

I. Data Flow and Event Information

With so much information available in a numerical relay, the question is: which event report is the correct one? Available fault data in a relay depends largely on the memory space and the type of protection element. Fig. 1 shows the most important items in a typical data flow diagram of a numerical relay. After the anti-aliasing low-pass filter and analog-to-digital conversion, the relay calculates the magnitude and phase of the current inputs. Because the anti-aliasing filter only attenuates higher frequencies, the signals still contain all frequencies and direct current value up to the cutoff frequency of the anti-aliasing filter.

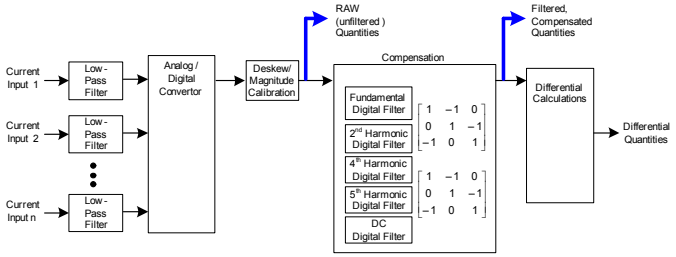

Fig. 1. Typical Data Flow Diagram of a Numerical Relay

In Fig. 1, these quantities are labeled RAW (unfiltered) Quantities, "unfiltered" referring to digital filtering. For the relay discussed in this paper, the sampling rate is 64 samples per cycle, with both filtered and raw data available at 64 samples per cycle, at 16 samples per cycle, at 8 samples per cycle, and at 4 samples per cycle. Which one to choose? Fig. 2 shows a composite signal containing fundamental, second-harmonic, third-harmonic, fourth-harmonic, and fifth-harmonic values.

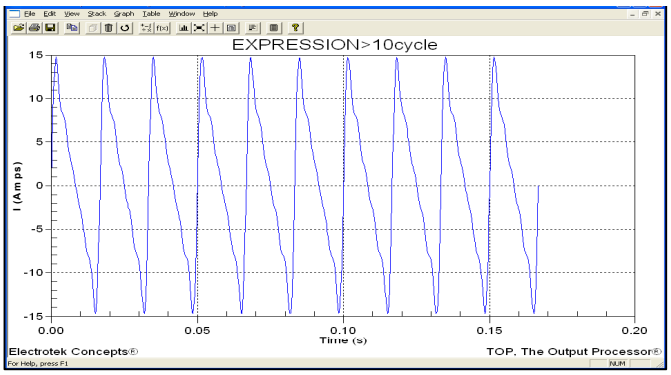

Fig. 2. TOP Generated Waveform

Fig. 3 shows the event report of the 16 samples-per-cycle RAW data. Clearly, the signals are closely correlated, in other words, the raw event report data contain substantially the same information as the applied signal.

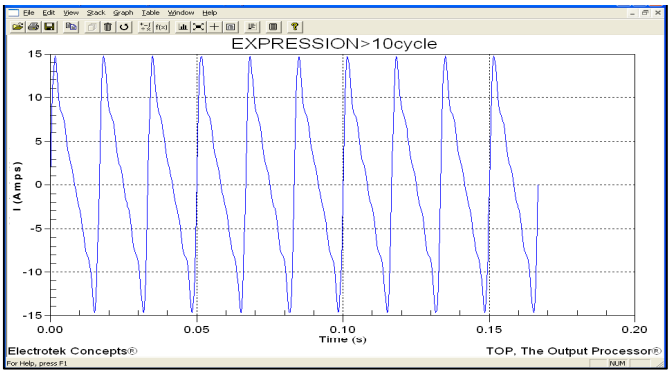

Fig. 3. Raw, 16 Samples-per-Cycle Event Report

Fig. 4 depicts the frequency analysis of the signal, showing the fundamental frequency (60 Hz) and the magnitudes of the second harmonic, third harmonic, fourth harmonic, and fifth harmonic as percentages of the fundamental.

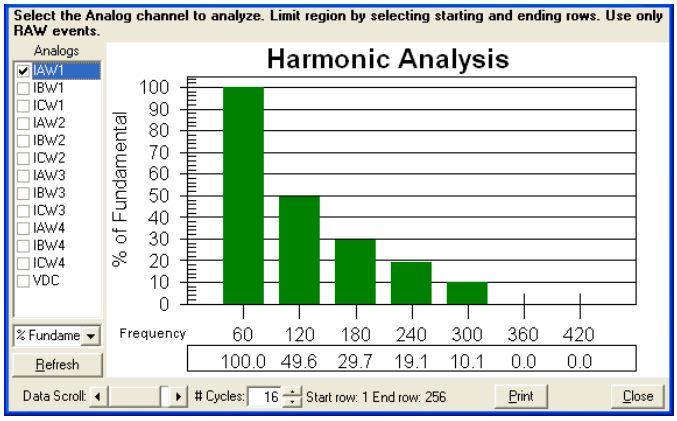

Fig. 4. Harmonic Contents of the Raw Signal

Fig. 5 shows the event report of the four samples-per-cycle, filtered data. By contrast, the filtered data contain only the fundamental frequency information.

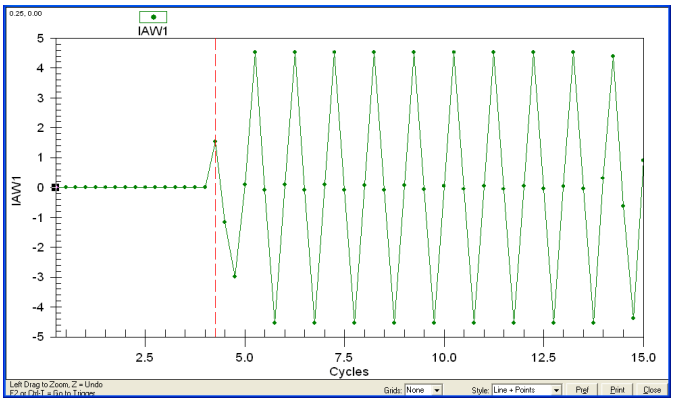

Fig. 5. Filtered, Four Samples-per-Cycle Event Report

Fig. 6 depicts the frequency analysis of the signal, showing only the fundamental frequency (60 Hz) information.

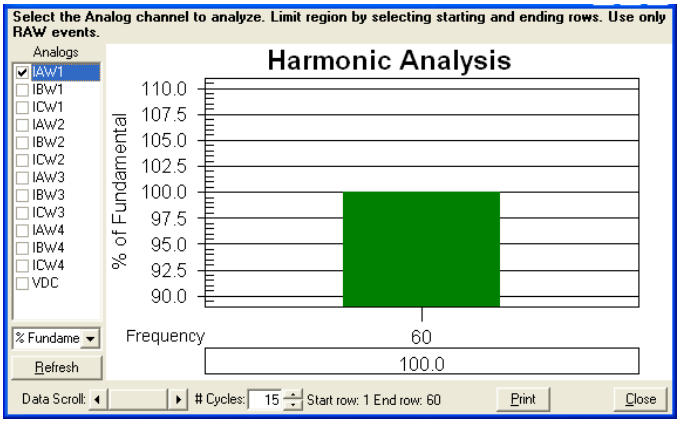

Fig. 6. Harmonic Contents of the Filtered Signal

II. Compensation

In addition to filtering, the relay further compensates for the phase-angle difference between the high-voltage winding (HV) and the low-voltage winding (LV) (see Appendix A), and removes zero-sequence currents if necessary (see Appendix B). Because standard CT ratios seldom match the full-load current of the transformer, the relay adjusts each phase current to compensate for the ratio mismatch between installed CTs and the transformer full-load current by calculating a scaling factor called TAP, using (1).

$$TAP = k \bullet \frac{MVA \bullet 1000}{\sqrt{3} \bullet kV \bullet CTR} \quad (1)$$

where:

k = 1 for wye-connected CTs, or k = √3 for delta-connected CTs

MVA = transformer rating in MVA

kV = system-rated voltage in kV

CTR = CT ratio (normalized)

The relay then uses the filtered, compensated quantities to calculate the per-unit values for use in the differential element. Table 1 shows the differences between the raw quantities and the filtered, compensated fundamental quantities.

TABLE 1
RAW QUANTITIES AND FILTERED, COMPENSATED FUNDAMENTAL QUANTITIES COMPARISON

Values	Raw Quantities	Filtered, Compensated Fundamental Quantities
Fundamental frequency	Yes	Yes
Harmonics	Yes	No
DC offset	Yes	No
Positive-sequence	Can be calculated*	Can be calculated
Negative-sequence	Can be calculated*	Can be calculated
Zero-sequence	Can be calculated*	No
Angle compensation	Can be calculated*	Yes

* After appropriate filtering and magnitude calculations

Raw data contain crucial information for analyzing CT performance. Such information is important because CT saturation poses the biggest problem for a correctly commissioned differential relay. In particular, the higher the amount of decaying dc present in the primary current, the higher the likelihood that CTs will saturate for prolonged through faults. Because the dc component is filtered out of filtered data, this vital dc information is lost to the analyst.

It is sometimes useful to test relay performance with different relay settings by injecting the fault event into the relay, usually in the IEEE Std. C37.111-1999 COMTRADE format. Most modern analysis software generates COMTRADE files when running the fault event, so that COMTRADE files are readily available. However, these COMTRADE files are only useful if generated from the RAW data. For example, Table 1 shows that there is no second harmonic present in the filtered data, but most modern transformer relays use the second harmonic to prevent differential operation during inrush conditions. Injecting the relay with a signal without the second harmonic may lead to incorrect conclusions.

Therefore, always select the RAW data at the highest sampling rate available in the relay for any fault analysis.

III. Differential Element Calculations

The final functional block in Fig. 1 is the differential element. As is the case with all protection elements, the operate/no operate decision is in the form of a comparator, comparing a measured quantity against a setting value. Fig. 7 shows such a comparator, which for the purpose of this discussion, we will call the differential comparator. When doing fault analysis, it is important to understand that the trip/no trip decision is not a comparison between the restraint current and operate current, but between two operate currents, namely, a measured operating current and an operating current calculated from the relay settings.

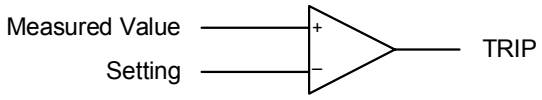

Fig. 7. Differential Comparator, Comparing a Measured Value Against a Setting

Equation (2) shows a typical form of the equation that the relay uses to calculate the measured quantity (operating current) for a two-winding transformer differential protection application.

$$IOPm = \left|\overline{I1} + \overline{I2}\right| \tag{2}$$

where:

IOPm = Measured operating current

I1 = Phasor current from Winding 1

I2 = Phasor current from Winding 2

For the setting value, the relay solves for the operating current as a function of the relay characteristic and the particular settings. Fig. 8 shows a single-slope differential characteristic.

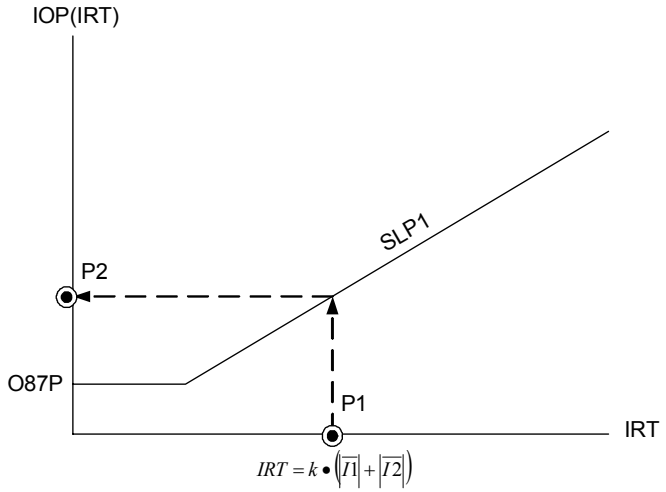

Fig. 8. Single-Slope Differential Element

Point P1 is the restraint current for specific values of I1 and I2 during any processing interval [see (3)]. Point P2 is the result of solving a straight-line equation with the specific IRT value [see (4)]. To start the calculations for the setting value, the relay uses (3) to calculate IRT, the independent variable in Fig. 8.

$$IRT = k \bullet \left(\left|\overline{I1}\right| + \left|\overline{I2}\right|\right) \tag{3}$$

where:

IRT = Restraint current

k = Design constant (usually 1 or 0.5)

I1 = Phasor current from Winding 1

I2 = Phasor current from Winding 2

Because the single-slope characteristic is a straight line starting at the origin, the relay uses (4) to solve for IOP(IRT) the setting value.

$$IOP(IRT) = SLP1 \bullet IRT \tag{4}$$

where:

IOP(IRT) = Solved operating current

SLP1 = Slope 1 setting

IRT = Restraint current [result from (3)]

For example, assuming that the CT ratios match the full-load current of the transformer (TAP1 = TAP2 = 1), determine whether the relay operates under the following condition:

SLP1 = 0.3 (30 percent)

$I1 = 5\angle 0°$

$I2 = 4\angle 150°$

k = 0.5

Use (2) to calculate IOPm as follows:

$$IOPm = \left|\overline{I1} + \overline{I2}\right| = \left|5\angle 0° + 4\angle 150°\right|$$

IOPm = 2.52 per unit

Use (3) to calculate IRT as follows:

$$IRT = k \bullet \left(\left|\overline{I1}\right| + \left|\overline{I2}\right|\right) = 0.5(4 + 5)$$

IRT = 4.5 per unit

Use (4) to calculate IOP(IRT) as follows:

$$IOP(IRT) = SLP1 \bullet IRT = 0.3 \bullet 4.5$$

IOP(IRT) = 1.35 per unit

Fig. 9 shows the comparator that compares IOPm and IOP(IRT). In this case, IOPm (2.52) is greater than IOP(IRT) (1.35) and the TRIP output asserts.

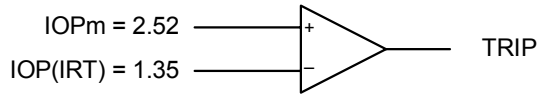

Fig. 9. Differential Element Comparator With TRIP Values

Furthermore, it is important to understand that event reports show the measured value (IOPm) and the restraint value (IRT), not IOP(IRT). Fig. 10 shows the magnitudes of the operate current (IOP1, bottom signal) and the restraint current (IRT1, top signal) of Differential Element 1. In Fig. 10, the restraint current (1.25 per unit) is much greater than the operating current (0.5 per unit). It may seem that the relay should not operate because the restraint current is larger than the operate current.

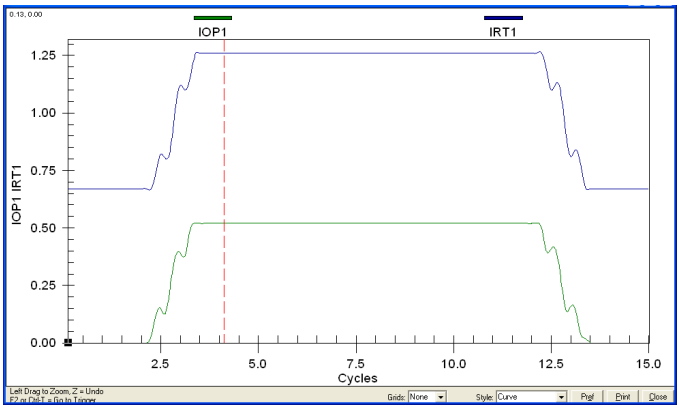

Fig. 10. Operate and Restraint Current Magnitudes

However, as discussed, the differential comparator compares IOPm and IOP(IRT). Notice that Fig. 10 shows IOPm and not IOP(IRT). It is still necessary to calculate IOP(IRT) using IRT and the slope setting before the differential comparator can make the trip/no trip decision. Therefore, for a SLP1 setting of 0.25 (25 percent), use (4) to calculate IOP(IRT), the setting value:

$$IOP(IRT) = SLP1 \bullet IRT = 0.25 \bullet 1.25$$

$$IOP(IRT) = 0.31 \text{ per unit}$$

Because the measured value (IOPm = 0.5 per unit) is greater than the setting value (IOP(IRT) = 0.31), the relay trips.

IV. Using Event Oscillography to Analyze Transformer Faults

Although analysis software is useful, all relevant relay information is not always available for manipulation in the analysis software. For clearer visual representation of the data, the following analysis uses a MathCAD™ worksheet that mimics the relay algorithms both in calculations and in data processing sequence. In general, the following discussion follows the data flow as depicted in Fig. 1. However, instead of first developing the relay operations and later applying these calculations to analyze system faults, we show the function block together with a graph.

To provide data for the graphs, we consider a case where a transformer differential relay operated for an external fault on the HV side (220 kV system) of the transformer. The fault occurred on one of the 220 kV feeders; the feeder breaker opened approximately four cycles after fault inception. Approximately three cycles after the feeder breaker tripped, the transformer breakers tripped. The customer stated that the feeder fault was a phase-to-phase fault. Fig. 11 is a capture of the raw event report that we will use for analyzing this fault.

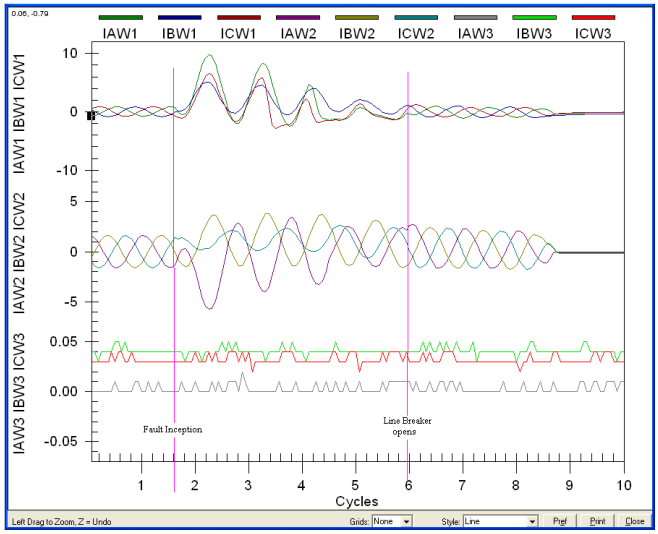

Fig. 11. Unfiltered (raw) Oscillographic Event Report of the Fault to be Analyzed

Fig. 12 is a single-line diagram of the customer's network and fault location. The transformer data are as follows:

Rating: = 120 MVA
Windings: = 3
Connections: = Wye/Wye/Delta [Star/Star/ Delta]
Voltage ratio: = 220/110/10.5 kV

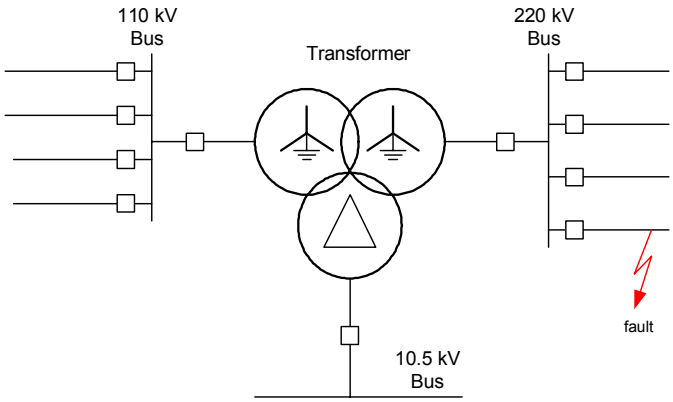

Fig. 12. Substation Single-Line Diagram

Although this is a three-winding transformer, the tertiary was unloaded and CT data are only available from the HV and LV windings. Although the tertiary was unloaded and played no visible function, it greatly influenced the fault current seen on the LV side of the transformer.

In order to analyzing the actual fault, we need more information regarding the data flow/processing path within the relay. Whereas Fig. 1 provides an overall view of the data flow in a numerical transformer relay, Fig. 7 gives more detailed information about the differential element. Fig. 13 also includes six references (a through f) to clearly show points where specific data observations apply.

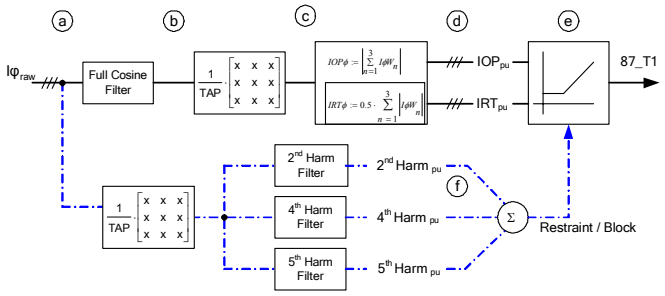

Fig. 13. Data Path in a Numerical Transformer Differential Relay

Starting with the unfiltered or raw data stored in the oscillographic event report, Fig. 14 (A) shows the unfiltered HV currents and Fig. 14 (B) shows the LV line or transformer terminal current. These currents are generated at point "a" in the data path in Fig. 13.

(A)

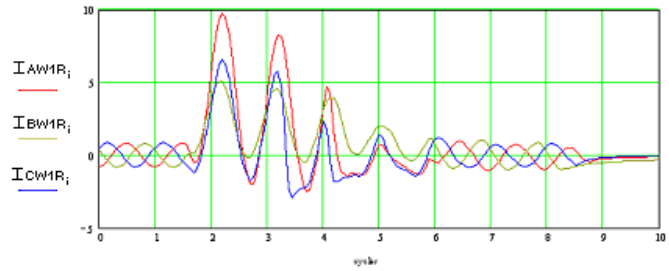

(B)

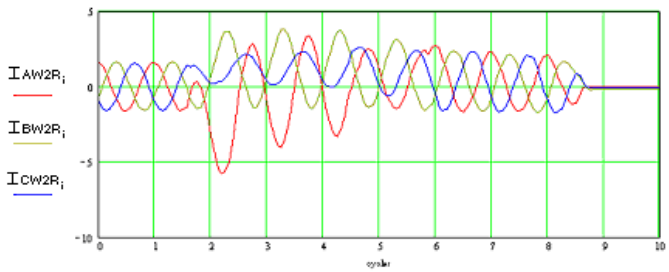

Fig. 14. HV Winding Unfiltered (raw) Phase Current (A) and LV Winding Unfiltered (raw) Phase Current (B)

Although the raw quantities provide extremely useful information such as dc-offset and waveform distortion, the next step is to filter the raw quantities in order to calculate the operating and restraint quantities. This particular relay uses a full-cycle cosine digital filter. Fig. 15 shows the filtered HV and LV winding currents. Note that filtering removes the dc offset and all nonfundamental frequency (harmonics) currents. These currents are generated at point "b" in the data path in Fig. 13.

(A)

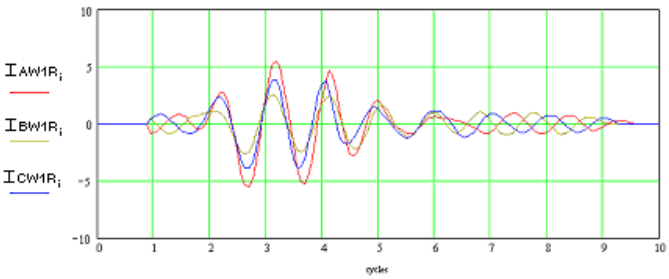

(B)

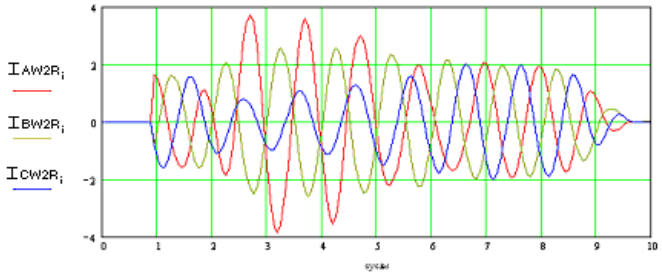

Fig. 15. HV Winding Filtered Phase Current (A) and LV Winding Filtered Phase Current (B)

Because the prime concern of the analysis is with the differential element operation, first consider the top path in Fig. 13, namely the calculation of the operating, restraint, and differential quantities. Fig. 16 shows the HV and LV currents after these currents have been filtered, scaled (TAP calculation), and phase corrected (matrix calculation). For these currents, refer to point "c" in Fig. 13.

(A)

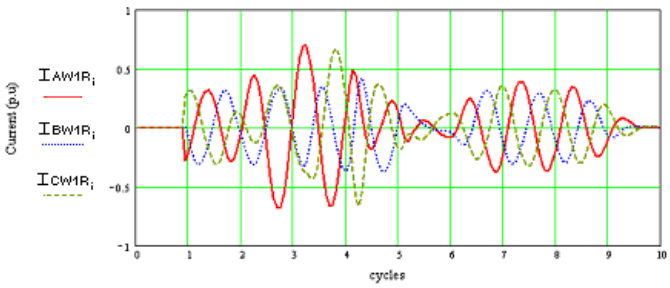

(B)

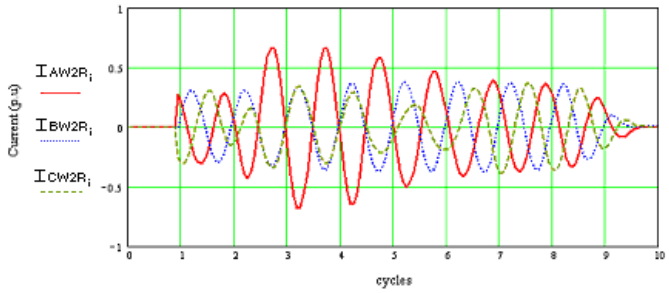

Fig. 16. HV Winding Currents After Filtering, and Magnitude and Phase Correction (A) and LV Winding Currents After Filtering, and Magnitude and Phase Correction (B)

An important aspect of transformer differential protection is that the differential elements operate on an effective differ-

ential element basis, and not on a transformer winding/phase basis (see Appendix A). For example, in a wye-connected winding, the line and phase currents are the same, but in a delta-connected winding, the line currents are the difference between two phase currents. Therefore, the relay does not compare the current in the transformer HV winding A-phase current to the LV current in the A-phase LV winding, but rather the current entering the A-phase differential element from the HV CTs against the current entering A-phase differential element from the LV CTs.

Recall that the transformer under consideration is a wye/wye/delta transformer. [1] For the two wye/wye windings, the compensation matrices must have the same elements (W1CTC = W2CTC = 1). With this compensation matrix selection, the input current for the A-phase differential element from the HV winding is composed of the currents from the A- and B-phase terminals (IA – IB). Fig. 17 shows the combination of HV currents and LV currents for the A-phase differential element. Therefore, the A-phase differential element calculates a differential current between a particular combination of currents from the HV winding and a particular combination of currents from the LV winding. The B- and C-phase differential elements have compositions similar to the A-phase differential element, using the appropriate current combinations.

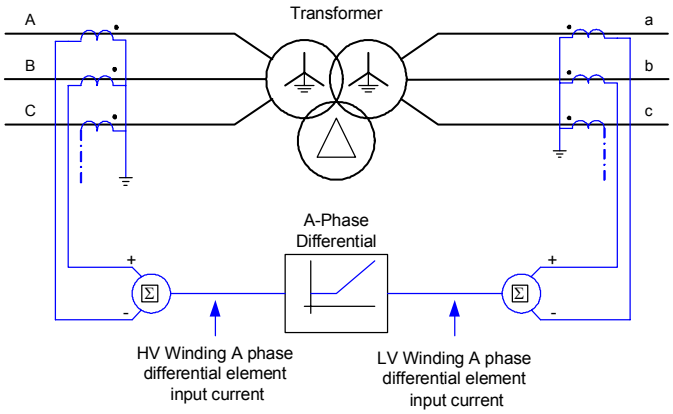

Fig. 17. Composition of the HV and LV Winding A-Phase Differential Element Input Current

Because the differential elements are a combination of particular currents, we have to examine all differential elements, and not any individual element on its own. Fig. 18, Fig. 19, and Fig. 20 show the HV winding differential input current and the LV winding differential input currents that make up the individual phase differential elements.

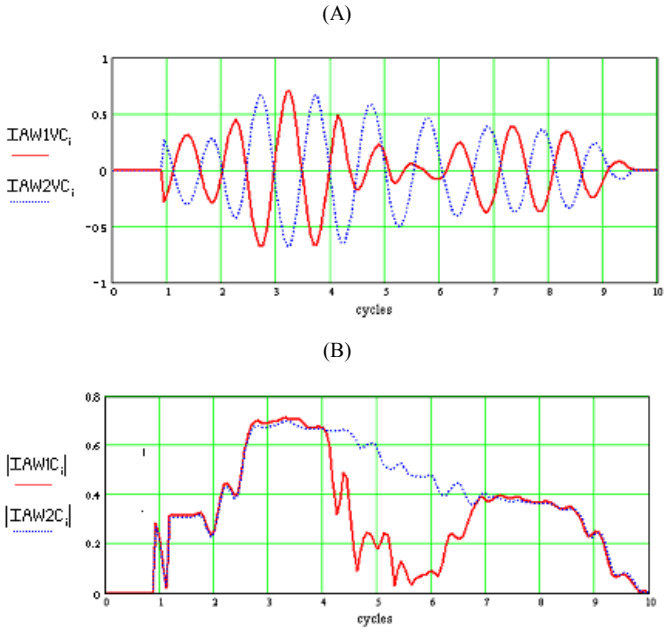

Fig. 18. A-Phase Differential Element Input Currents (A) and A-Phase Differential Element Input Current Magnitudes (B)

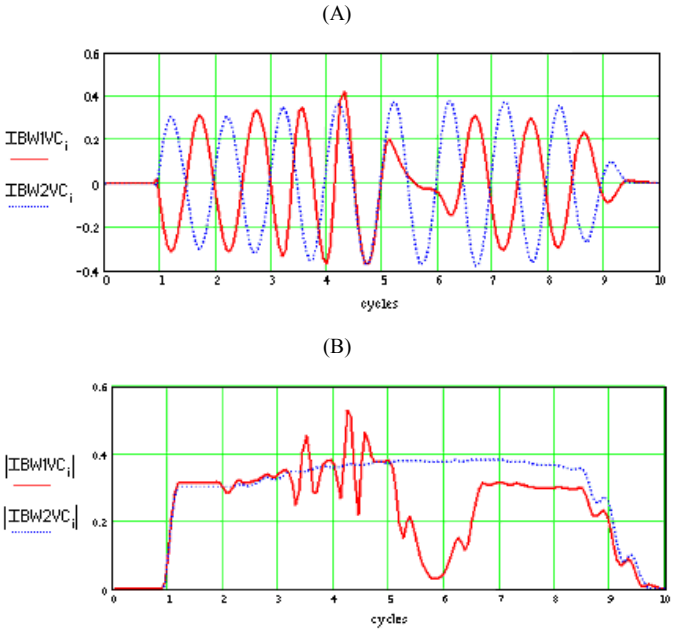

Fig. 19. B-Phase Differential Element Input Currents (A) and B-Phase Differential Element Input Current Magnitudes (B)

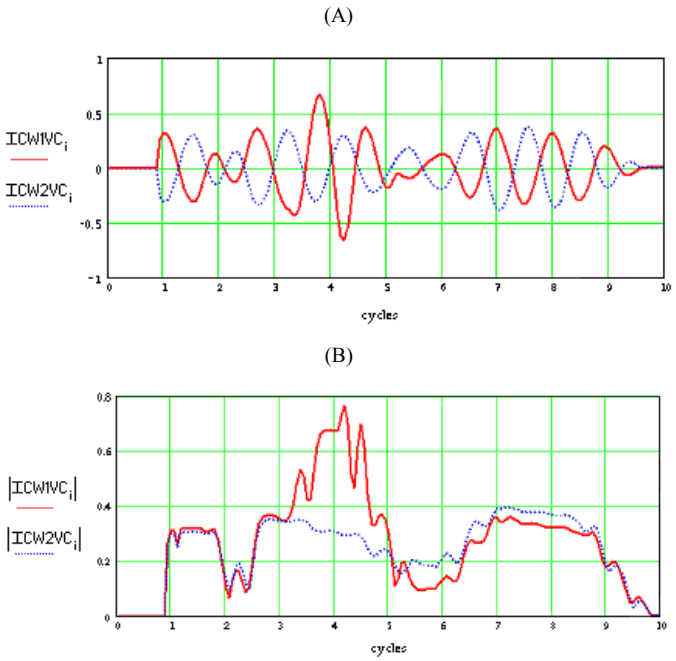

Fig. 20. C-Phase Differential Element Input Currents (A) and C-Phase Differential Element Input Current Magnitudes (B)

For steady-state values, Fig. 18, Fig. 19, and Fig. 20 are most useful because these graphs clearly show whether the magnitude and angle compensation (and thus the matrix selection for the particular transformer-vector group) are correct. These graphs also provide the operate and restraint currents necessary for fault analysis. From examining the raw current graphs (Fig. 14), it is clear that the fault inception occurred at approximately 1.6 cycles. This correlates with the graphs of the differential elements (Fig. 18, Fig. 19, Fig. 20) and the original oscillographic event (Fig. 11) because we see a change in the current magnitude in the different differential elements. From Fig. 18, Fig. 19, and Fig. 20, we see an increase of equal magnitude in both HV winding currents and LV winding currents and these currents are 180° out of phase. This is typical for an external fault. However, on close inspection of the phase angle between the HV winding differential element input current and the LV winding differential element input current at approximately cycle 3, the phase angle between the two input quantities changes from being 180° out of phase to being in phase. Can we conclude that the fault evolved at approximately cycle 3 from an external fault into an internal fault? Fig. 21 (enlarged graph of Fig. 19 between cycles 3.5 and 6.5) shows that the input currents into the differential element are in phase, a clear indication of an internal fault.

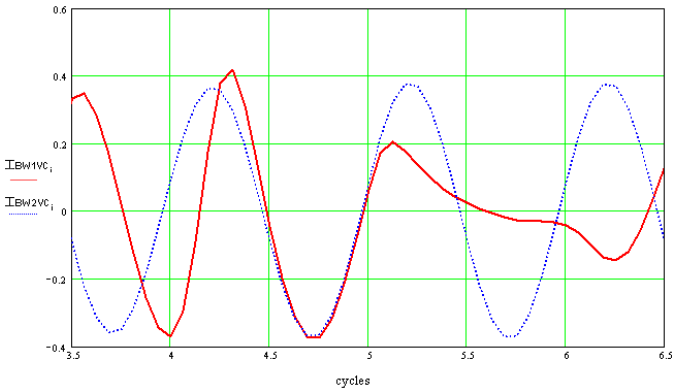

Fig. 21. Zoomed Graph of the B-Phase Differential Element Input Currents

The A-phase differential elements inputs currents exhibit similar traits as that of the B-phase, albeit not as severe.

However, looking at the raw current waveforms (Fig. 22) there is no evidence of this current inversion. Why this apparent contradiction?

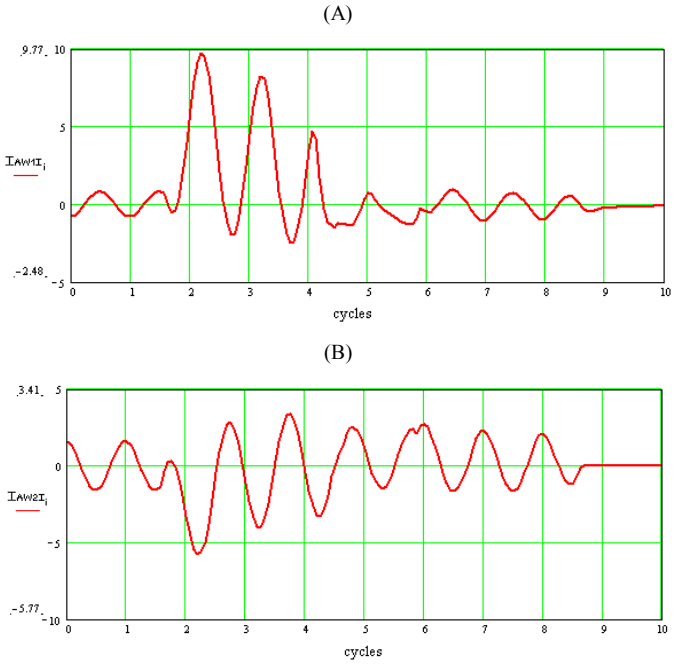

Fig. 22. HV Winding unfiltered A-Phase Current (A) and LV Winding Unfiltered A-Phase Current (B)

In analyzing the raw current waveform of the HV winding A-phase, beginning at the time of fault inception, we can make the following observations:

- At fault inception the current is sinusoidal with a dc offset
- At cycle 3.5 the current distortion starts
- From cycle 4 to cycle 6 the current is severely distorted and has decreased in magnitude
- After cycle 6 the current is sinusoidal

During the same time interval, the LV winding raw-current waveforms appear to remain sinusoidal except for some slight distortion between cycles 4.5 to 6.

Clearly, the period of interest is between cycle 3.5 and cycle 6. During this time, the HV winding A-phase shows severe distortion because of CT saturation. To substantiate this claim,

we investigate the second- and fourth-harmonic content of the HV winding A-phase current. Fig. 23 shows the second- and fourth-harmonic content of the A-phase line current for both the HV and LV winding.

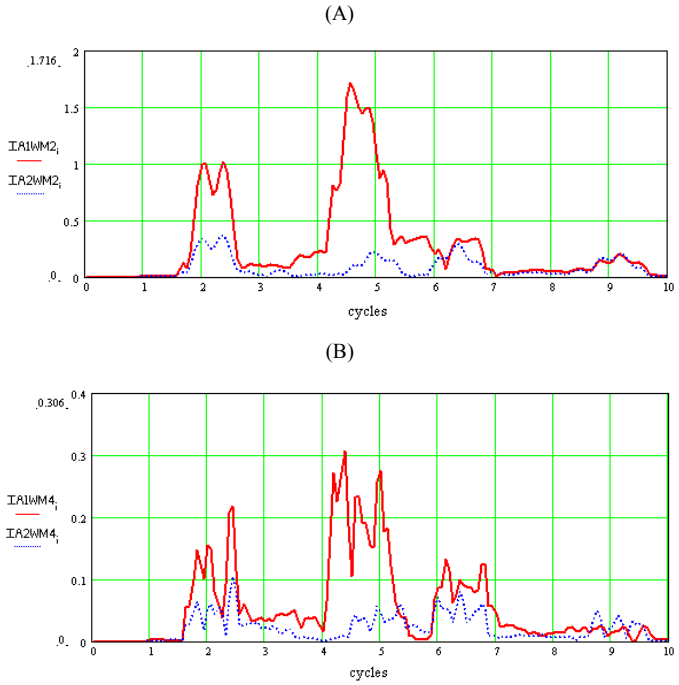

Fig. 23. A-Phase Second- and Fourth-Harmonic Content of the HV Winding A-Phase Current (A) and A-Phase Second- and Fourth-Harmonic Content of the LV Winding A-Phase Current

Analyzing the second- and fourth-harmonic plots, we can make the following observation:

- There are no second or fourth harmonics present in either the HV or LV currents prior to the fault.
- At fault inception, there is an increase in both second and fourth harmonics in both the HV and LV windings.
- At approximately cycle 3.5, the second harmonic begins to increase in the HV winding, reaching a maximum value at approximately cycle 5. The LV winding current does not experience the same increase in second-harmonic current as the HV winding does.
- At approximately cycle 4, the fourth harmonic begins to increase in the HV winding, reaching a maximum value at approximately cycle 4.5. Again, the LV winding current does not experience the same increase.

From the second- and fourth-harmonic analysis (HV and LV winding A-phase currents), we observe that the HV winding CT experienced increases in second- and fourth-harmonic content during cycles 3.5–6. During the same time, there was no increase in the second- and fourth-harmonic contents of the LV winding CT. From these observations, we conclude that the HV winding CT saturated during this time period.

If we now analyze the B-phase unfiltered winding currents, shown in Fig. 24, we see that these currents remain nearly sinusoidal. The only exception seems to occur approximately between cycle 5 and cycle 6 on the HV winding current. The LV winding current remains sinusoidal during the entire fault.

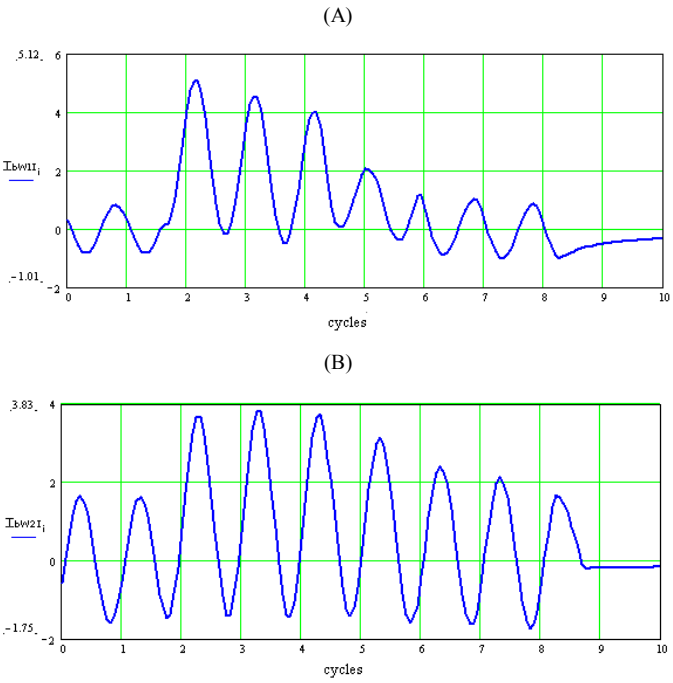

Fig. 24. HV Winding Unfiltered B-Phase Current (A) and LV Winding Unfiltered B-Phase Current (B)

Computing the second- and fourth-harmonic contents of the HV and LV line currents, shown in Fig. 25, we can make the following observations:

- The second-harmonic content of the HV winding current increases sharply at fault inception, then decays within 1 cycle, and increases again at approximately cycles 5 and 7. The LV winding current has a very low second-harmonic content.
- There is very little fourth-harmonic content in both HV and LV winding currents.

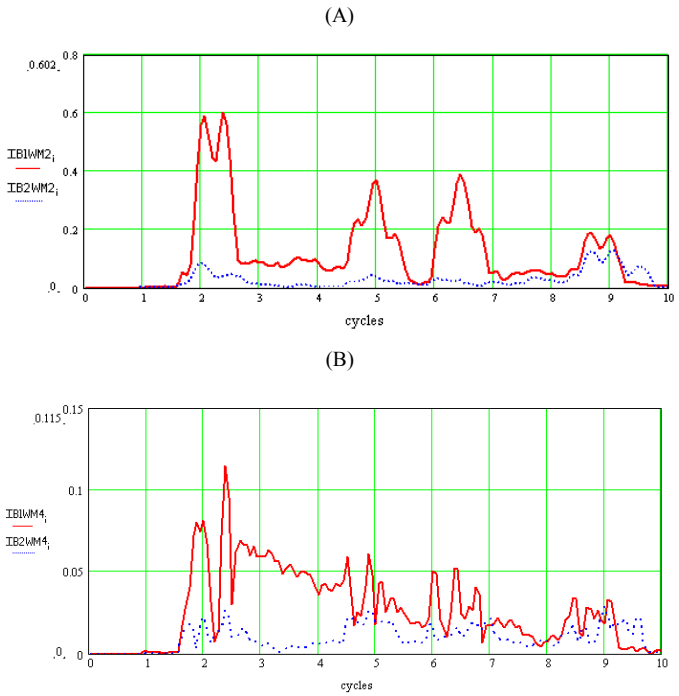

Fig. 25. Second- and Fourth-Harmonic Contents of the HV Winding B-Phase Current (A) and Second- and Fourth-Harmonic Contents of the LV Winding B-Phase Current (B)

From the above analysis we conclude that the B-phase HV winding CT experienced slight saturation during cycles 5–6, but the B-phase LV winding CT did not experience any saturation.

Finally, from analyzing the HV winding C-phase currents and the unfiltered currents as shown in Fig. 26 (A), we conclude the following:

- At fault inception the current is sinusoidal with a dc offset
- At approximately cycle 3.2, the waveform does not remain completely sinusoidal
- From cycle 3.5 to cycle 6 we see that the waveform is no longer sinusoidal and has decreased in magnitude
- After cycle 6 the waveform once more becomes sinusoidal

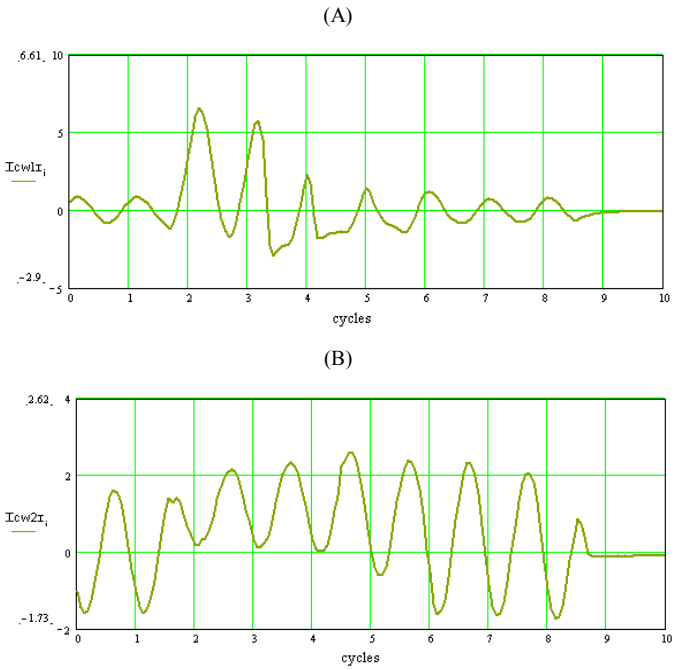

Fig. 26. HV Winding Unfiltered C-Phase Current (A) and LV Winding Unfiltered C-Phase Current (B)

If we examine and analyze LV winding C-phase raw current waveforms, these waveforms appear to remain sinusoidal except for the dc offset from the onset of the fault. The period of interest seems to be between 3.2 to 6 cycles. During this time we can say the HV winding C-phase CT went into saturation. To substantiate this claim, we will compute the second- and fourth-harmonic content of the HV winding C-phase current. Fig. 27 shows the second- and fourth-harmonic content of the C-phase line current for both the HV and LV winding.

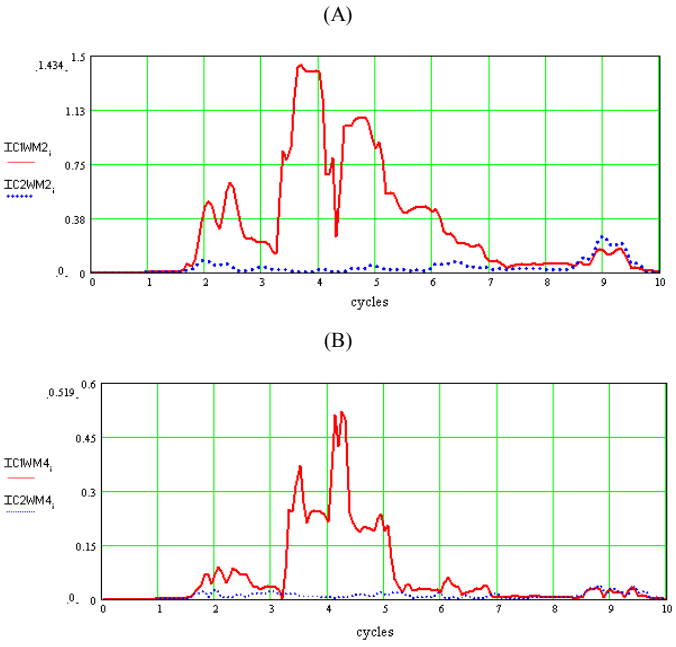

Fig. 27. Second- and Fourth-Harmonic Content of the HV C-Phase Current (A) and Second- and Fourth-Harmonic Content of the LV C-Phase Current (B)

Analyzing the second- and fourth-harmonic plots, we can make the following observation:

- Prior to the fault, there is no second or fourth harmonics present in either the HV nor LV currents.
- At fault inception, there is an increase in the second harmonic in both the HV and LV winding.
- The fourth-harmonic content does not change significantly in either winding.
- At approximately cycle 3.2 the second harmonic begins to increase in the HV and LV windings. In the HV winding the second harmonic reaches its peak value at approximately cycle 3.8. The LV winding current does not experience the same excursion of second-harmonic current as the HV winding does.

At approximately cycle 4.2 the second harmonic of the HV winding decreases sharply for approximately 0.2 cycles before recovering

As an overall statement, we can say the HV CTs experienced saturation in varying degrees, with the B-phase CT experiencing some saturation and the A- and C-phase CTs experiencing quite severe saturation.

Although we now have enough information to examine the operation of the individual differential elements, the cause of the dissimilar CT saturate is still unknown. We will answer this question a little later; for now we will concentrate on why the differential element misoperated.

Recall that the A-phase differential element current inputs consist of the A-phase and the B-phase line currents for both the HV and LV windings. To see what effect the saturation of the A-phase HV line current has on the A-phase differential element, let us examine the A-phase differential element in detail. Fig. 11 showed the inputs into the A-phase differential elements. Fig. 28 shows the calculated operate and restrained currents derived from the input currents; these quantities can be observed at point "d" in Fig. 13.

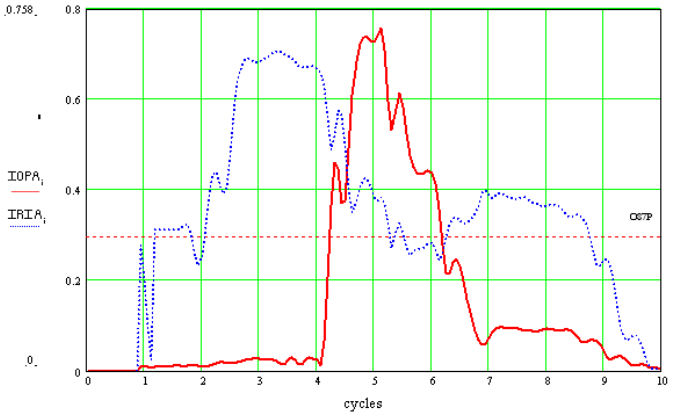

Fig. 28. A-Phase Differential Element Calculated Operate and Restrained Currents

From Fig. 28, we can see that before the fault, in cycles 1–1.6 the restraint current is about 0.32 per unit and the operate current is approximately zero, a normal condition for an unfaulted, loaded power transformer. At fault inception, (cycle 1.6 to cycle 4), the operate current remains approximately at zero while the restraint current increases to approximately 0.7 per unit. At cycle 4, the restraint current begins to decrease and the operate current begins to increase; this corresponds to the time when the A-phase HV CT begins to saturate. At cycle 5, the operate current is nearly twice the restraint current. This is a result of the output of the HV line CT being nearly zero. This means that the operate and restraint currents of the A-phase differential element are composed solely from the LV line current. The operate and restraint currents are calculated as shown in (2) and (3) where k = 0.5 in (3).

At approximately cycle 6, the feeder breaker clears the fault and we see that the CT begins to pull out of saturation. Fig. 21 also shows the CT pulling out of saturation, in other words, when the restraint current begins to increase and the operate current begins to decrease. Notice that at cycle 7, the restraint current is larger than the operate current. However, the operate current is as yet not zero; this is because the HV A-phase line CT has not completely emerged from saturation.

Fig. 29 (A), (B), and (C) shows three "snapshots" over a 10-cycle period of the operate and restraint current of the differential element during the fault.

- Prefault and fault before the CTs saturate, Fig. 29 (A), 0–4 cycles
- During the fault with the CT saturated, Fig. 29 (B), 4–6 cycles
- Post fault when the CT pulls out of saturation, Fig. 29 (C), 6–10 cycles.

(A)

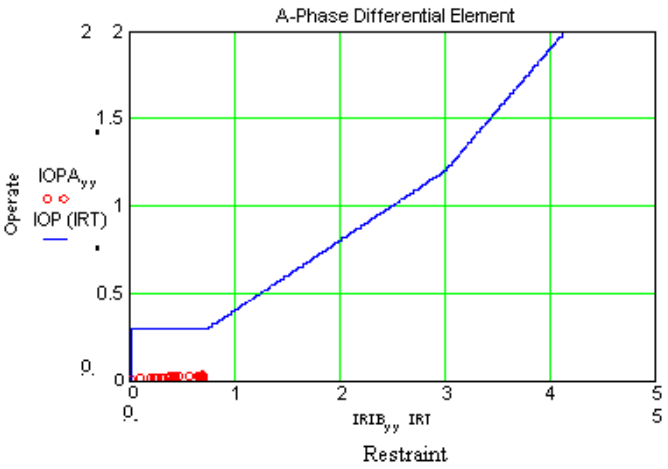

Cycles 0–4

(B)

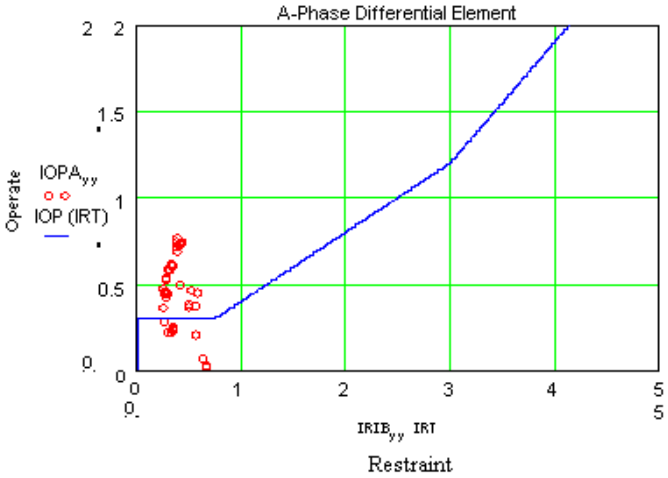

Cycles 4–6

(C)

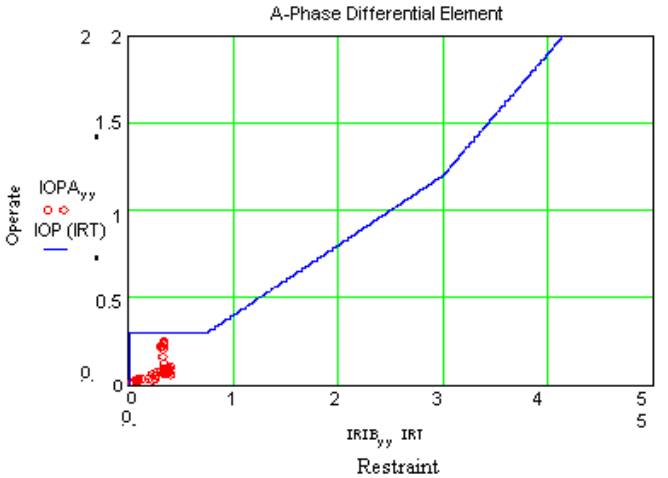

Cycles 6–10

Fig. 29. 10-Cycle Period of Operate and Restrain Current of Differential Element During Fault

Fig. 29 (A) shows a typical plot for an external fault or load condition in that the differential element plots into the restraint region. Fig. 29 (B) shows the migration of the operating point of the differential element from the restraint region into the operate region, resulting from the HV A-phase winding CT going into saturation. Fig. 29 (C) shows that, once the fault is cleared, the operating point of the differential element returns to the restraint region as the CT begins to pull out of saturation. Fig. 30 and Fig. 31 show the behavior of the B- and C-phase differential elements.

(A)

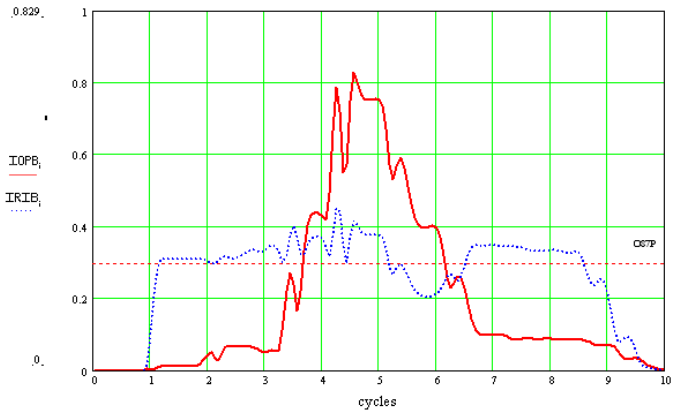

(B)

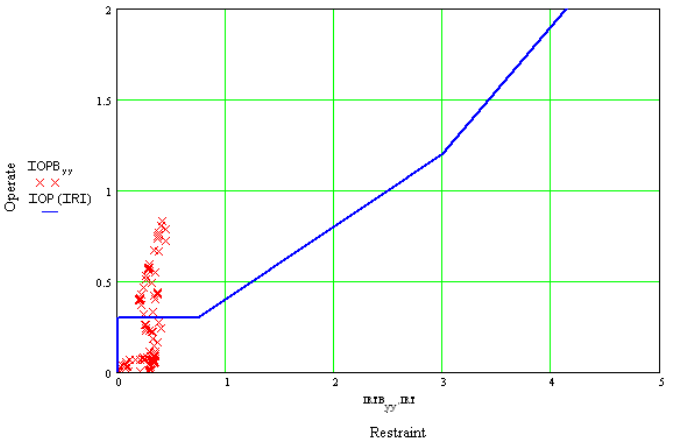

Fig. 30. B-Phase Differential Element Calculated Operate and Restrained Currents (A) and B-Phase Differential Element Restraint vs. Operate Currents

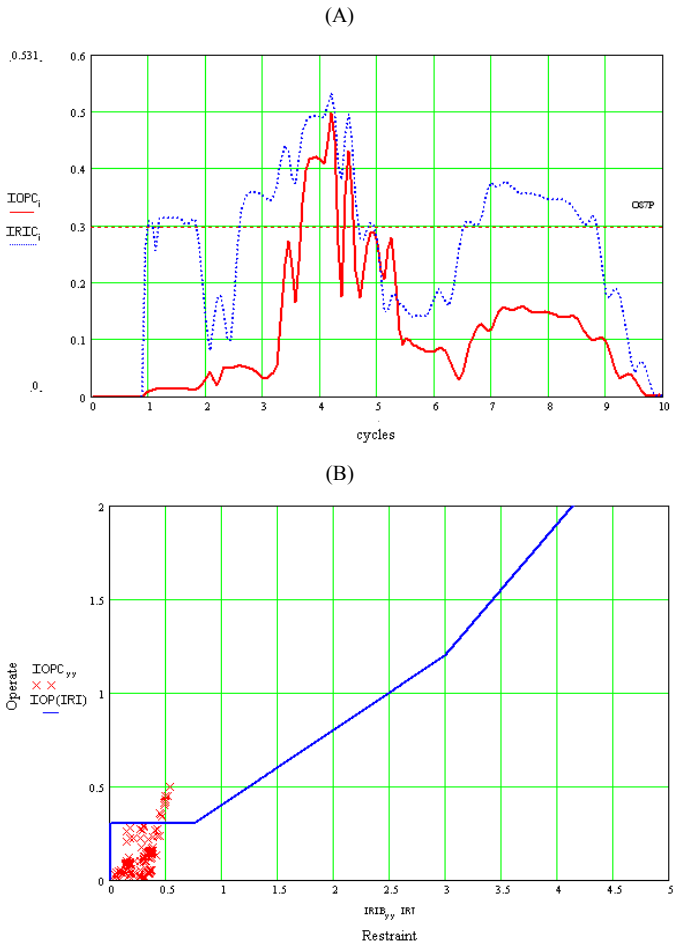

Fig. 31. C-Phase Differential Element Calculated Operate and Restrained Currents (A) and C-Phase Differential Element Restraint vs. Operate Currents (B)

One question that now comes to mind is why the operating point of the differential element has relatively low magnitudes while the fault currents are reasonably high. There is only one calculation that reduces the current: the removal of the zero-sequence component of the phase current. But for the effect to be substantial, the line currents must contain primarily zero-sequence current. Fig. 32 shows the sequence currents of the HV and LV winding sequence components.

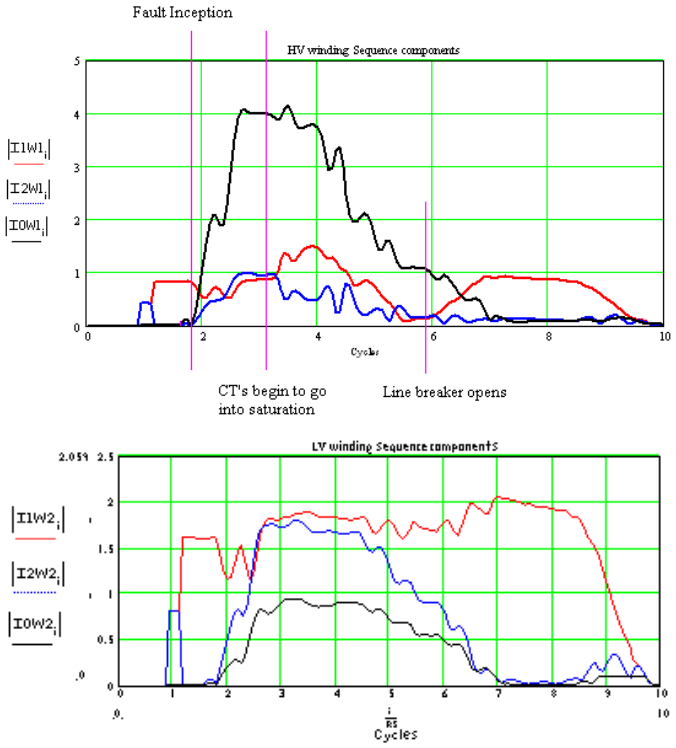

Fig. 32. Sequence Components in the HV and LV Windings

From Fig. 32, the zero-sequence current resulting from the fault and before the current transformer goes into saturation is nearly four times the positive-sequence and negative-sequence currents. From this information, we conclude that:

- The fault involves ground
- Strong zero-sequence source and relatively weak positive- and negative-sequence source

Note that when a current transformer goes into saturation it results in generating a non-real/fictitious zero-sequence current, therefore once a current transformer goes into saturation, the sequence data calculated using this information are no longer reliable.

On the LV winding, positive-sequence and negative-sequence currents are twice as large as the zero-sequence current. Why this discrepancy? What happened to the zero-sequence current? Recall that this is a three-winding transformer and that the third winding (delta connected) is a zero-sequence sink, so that the difference of the HV and LV winding zero-sequence current circulates in the tertiary winding. Fig. 33 is a sketch of the zero-sequence component diagram for this type of transformer winding configuration [2], [3].

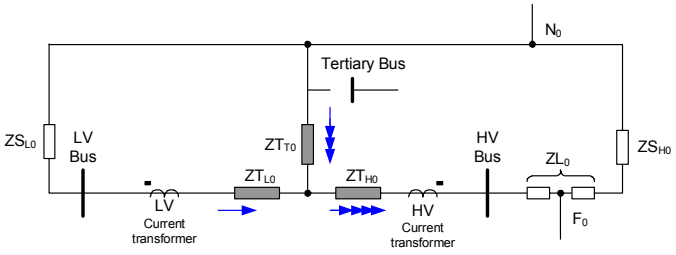

Fig. 33. Zero-Sequence Diagram for a Wye/Wye/Delta Connected Transformer

Referring to Fig. 33: even though there is no load connected to the tertiary winding, the tertiary winding sinks a great deal of zero-sequence current. Because no CT is installed in the delta winding, we cannot measure the current that actually flows in the delta winding during such a fault condition.

To further substantiate this claim, Fig. 34 shows the differential element plot for the A-phase differential element when the matrix compensation was set to that of a unit matrix, one in which no zero-sequence current removal occurs. (NOTE: this change of setting is only to substantiate the claim; do not select this setting on a grounded-wye winding; failure to remove the zero-sequence current from the differential elements will result in relay misoperation for out-of-zone ground faults).

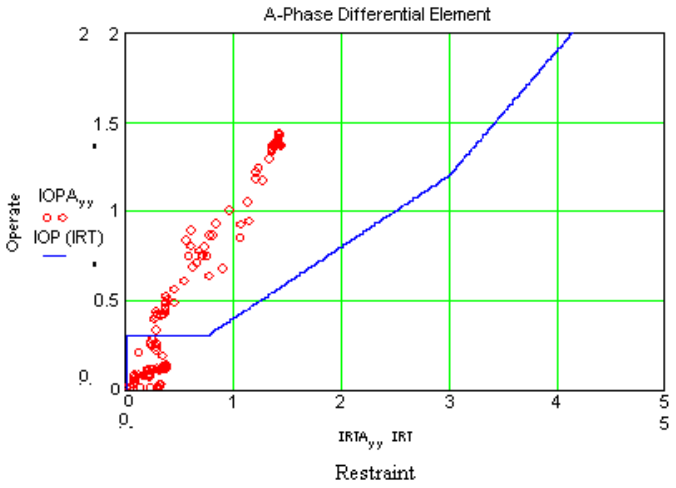

Fig. 34. A-Phase Differential Element Plot When Unit Matrix Compensation is Applied

From Fig. 34, we see that even with the unit matrix compensation, the differential element still migrated into the operating region. The only difference is that this time the magnitude of the excursion is greater.

To provide differential element stability during transformer energization, transformer differential elements use either harmonic blocking elements or harmonic restraint elements. Pursuing the lower path of Fig. 6, we can determine the harmonic current content of the unfiltered operating current. It is the content of this raw operating current that the relay uses to determine whether to restrain/block the differential element.

[4] In general, the relay also calculates the harmonics to restrain/block the differential element on a differential basis, i.e. subtracts the LV harmonics from the HV harmonics. This calculation is necessary to separate the harmonics generated in the load from the harmonics generated within the transformer. Note that the harmonic analysis in the previous section determined the harmonic content of the individual line phase current, and not in a differential calculation. Fig. 35 (A), (B) and (C) shows the second-, fourth-, and fifth-harmonic current content of the raw operating current for the A-, B-, and C-phase differential elements (differential calculations).

(A)

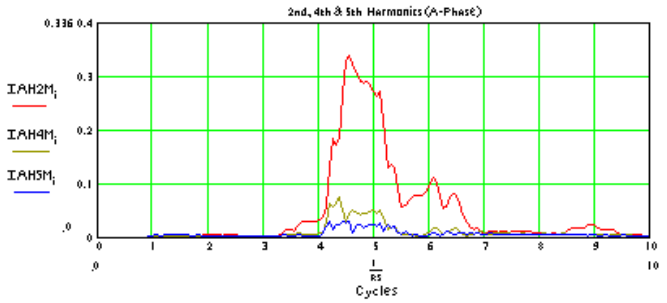

(B)

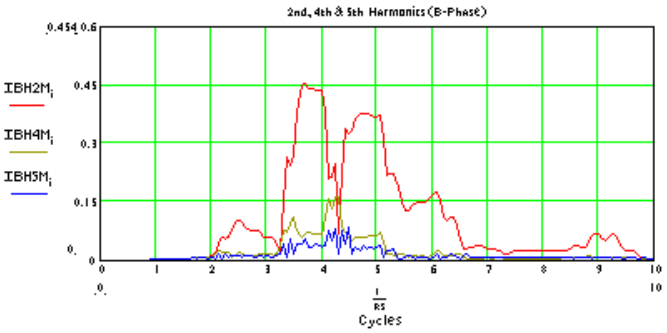

(C)

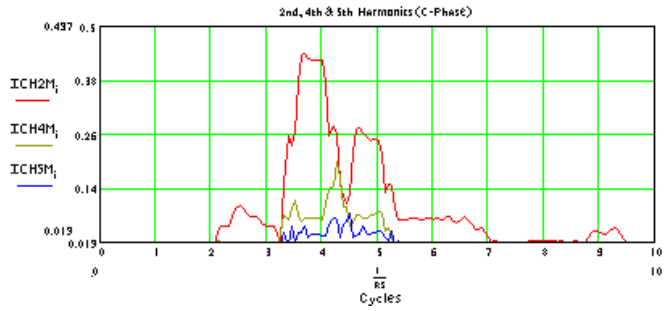

Fig. 35. Second-, Fourth-, and Fifth-Harmonic Current Content of the "Raw Operating" Current for A-, B-, and C-Phase Differential Elements

Fig. 35 shows that the B- and C-phase second- and fourth-harmonic content decreases sharply at approximately cycle 4 and only recovers approximately one-half cycle later. This is approximately the same time that the A- and C-phase CTs went into deep saturation.

V. Summary and Conclusion

This paper provided general information regarding current compensation and differential element calculations, followed by a step-by-step analysis of a transformer differential relay misoperation.

1. Using raw data provides valuable system information not available when considering only the filtered data. Always use the raw data at the highest available sampling rate for fault analysis.
2. Manipulate the data by means of mathematical programs such as MathCAD to emulate relay elements.
3. Analyzing event data at selected points of data manipulation in the relay isolates relay elements to perform discrete functional analysis on these individual elements. For

example, when the harmonic content of the fault current is analyzed discretely, we see that the harmonic content can vary considerably during the fault, especially if the current transformer goes into severe saturation. This considerable variation in the harmonic content of the fault current can lead to misoperation of the differential element.

VI. Appendix A

A. Phase-Angle Compensation

Phase-angle differences come about when one set of power transformer windings is wye connected, and the other set of windings is delta connected. For example, consider the YDAB (YNd11) connection shown in Fig. A1. If we take the A-phase of the HV winding as reference, the a-b delta connection causes the A-phase of the LV winding to differ by 30° with respect to the A-phase HV winding.

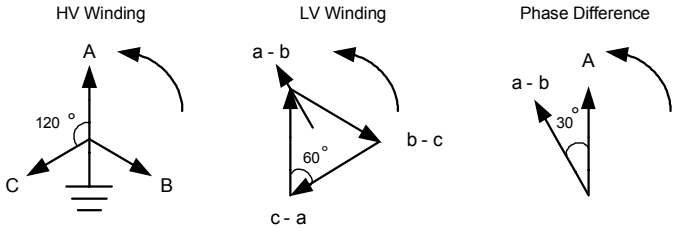

Fig. A1. Phase Shift Between HV and LV Sides of a YDAB (Ynd11) Transformer

With electromechanical relays, CTs from wye-connected power transformer windings are connected in delta, and CTs from delta-connected power transformer windings are connected in wye to compensate for this phase shift. When both HV and LV CTs are wye connected, CT connections cannot compensate for this 30° phase difference; the secondary current from the HV winding and the secondary current from the LV winding are phase shifted by 30°. For correct differential operation, we need to correct for the phase shift of wye-delta transformers in the relay software. To achieve this phase-shift correction, the relay mathematically forms the delta connection in the software. Equations (5) through (7) show the three line current equations for the YDAB transformer connection.

$$I_{ab} = I_a - I_b \quad (I_c = 0) \tag{5}$$

$$I_{bc} = I_b - I_c \quad (I_a = 0) \tag{6}$$

$$I_{ca} = I_c - I_a \quad (I_b = 0) \tag{7}$$

If (5) through (7) are in matrix format, the placeholders for the current vectors are as follows:

$$\begin{bmatrix} Ia & Ib & Ic \\ Ia & Ib & Ic \\ Ia & Ib & Ic \end{bmatrix} \text{ so that } I_{ab} = I_a - I_b \text{ becomes } \begin{bmatrix} 1 & -1 & 0 \end{bmatrix} \bullet \begin{bmatrix} Ia \\ Ib \\ Ic \end{bmatrix}$$

$(I_c = 0)$

Renaming $I_{ab} = I_{ACOMP}$, we complete the current relationships of the YDAB transformer in matrix form as follows (divide by $\sqrt{3}$ to correct the magnitude):

$$\begin{bmatrix} I_{A\,COMP} \\ I_{B\,COMP} \\ I_{C\,COMP} \end{bmatrix} = \frac{1}{\sqrt{3}} \begin{bmatrix} 1 & -1 & 0 \\ 0 & 1 & -1 \\ -1 & 0 & 1 \end{bmatrix} \bullet \begin{bmatrix} I_A \\ I_B \\ I_C \end{bmatrix}$$

In the same manner we form other "delta" matrices for transformer vector groups that require a 30° phase shift correction.

B. Vector-Group Compensation Using Matrix Algebra

A vector (or phasor) is a quantity with both magnitude and direction, as opposed to a scalar quantity which has magnitude only. In the rectangular form, we represent a vector as follows:

$$\vec{Z} = x + jy$$

where
Z = vector
x = real component
y = imaginary component
$j = \sqrt{-1}$

In the polar form, we represent a vector as follows:

$$\vec{Z} = |Z| \angle \theta$$

where

$$|Z| = \sqrt{x^2 + y^2}$$

$$\theta = \tan^{-1}\left(\frac{y}{x}\right)$$

We require only basic vector algebra to manipulate the vector quantities. For example, calculate the difference between IA and IB in Fig. A2.

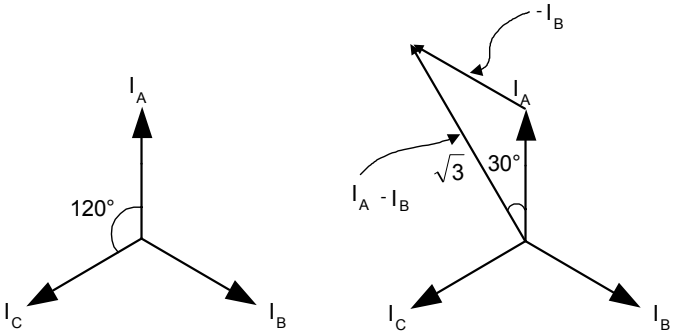

Fig. A2. Addition of Vector IA and Vector –IB

$$IA - IB = IA\angle 90° - IB\angle -30°$$

$$IAB = \sqrt{3}\angle 120°$$

By dividing IAB by $\sqrt{3}$, we have a vector with magnitude IA, but advanced by 30°. For example, to calculate the compensated values of three system currents (taking IA as reference), multiply the three system currents ($1\angle 0°$, $1\angle -120°$, and $1\angle 120°$) by matrix M1:

$$M1 = \begin{bmatrix} 1 & -1 & 0 \\ 0 & 1 & -1 \\ -1 & 0 & 1 \end{bmatrix}$$

$$\begin{bmatrix} I_{A\,COMP} \\ I_{B\,COMP} \\ I_{C\,COMP} \end{bmatrix} = \frac{1}{\sqrt{3}} \begin{bmatrix} 1 & -1 & 0 \\ 0 & 1 & -1 \\ -1 & 0 & 1 \end{bmatrix} \bullet \begin{bmatrix} 1\angle 0° \\ 1\angle -120° \\ 1\angle 120° \end{bmatrix}$$

$$\begin{bmatrix} I_{A\,COMP} \\ I_{B\,COMP} \\ I_{C\,COMP} \end{bmatrix} = \frac{1}{\sqrt{3}} \begin{bmatrix} 1\angle 0° & -1\angle 120° & 0 \\ 0 & 1\angle -120° & -1\angle 120° \\ -1\angle 0° & 0 & 1\angle 120° \end{bmatrix}$$

$$\begin{bmatrix} I_{A\,COMP} \\ I_{B\,COMP} \\ I_{C\,COMP} \end{bmatrix} = \frac{1}{\sqrt{3}} \begin{bmatrix} 1.73\angle 30° \\ 1.73\angle -90° \\ 1.73\angle -150° \end{bmatrix}$$

$$\begin{bmatrix} I_{A\,COMP} \\ I_{B\,COMP} \\ I_{C\,COMP} \end{bmatrix} = \begin{bmatrix} 1.0\angle 30° \\ 1.0\angle -90° \\ 1.0\angle -150° \end{bmatrix}$$

VII. Appendix B

Why eliminate zero-sequence current? Fig. B1 shows a wye-delta transformer with the wye winding grounded. Ground faults on the HV side of the transformer result in current flowing in the lines of the wye-connected windings, and therefore, the HV CTs. This current distribution is different in the LV windings of the transformer. Fault current for ground faults on the HV side of the transformer circulates in the delta-connected windings, but no current flows in the LV lines and, hence, no current flows in the LV CTs. Because fault current flows in the HV CTs only, the differential protection is unbalanced and can misoperate.

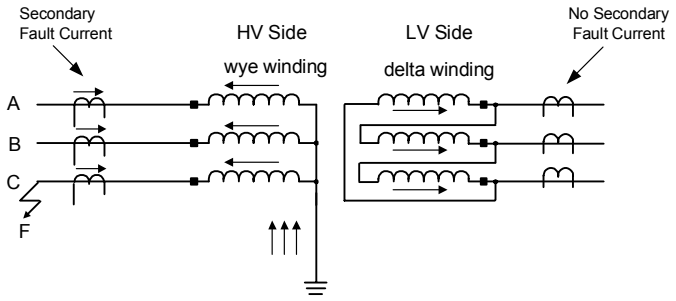

Fig. B1. YDAB Transformer

Clearly, we need to eliminate the zero-sequence from CTs connected to all grounded, wye-connected transformer windings. Because all CTs are wye connected, we need to remove the zero-sequence currents mathematically in the relay. One way to remove the zero-sequence current is by means of the delta matrices we use for phase-angle correction. For a DAB delta, connecting a–b, b–c, and c–a phases forms the delta connection. Of these three groups, consider the $I_a - I_b$ connection. Equations (8) and (9) express I_a and I_b in terms of symmetrical components, A-phase being the customary reference.

$$I_a = I_1 + I_2 + I_0 \tag{8}$$

$$I_b = \alpha^2 I_1 + \alpha I_2 + I_0 \tag{9}$$

$$I_a - I_b = I_1 + I_2 + I_0 \; - \alpha^2 I_1 - \alpha I_2 - I_0 \tag{10}$$

$$I_a - I_b = I_1\left(1 - \alpha^2\right) + I_2\left(1 - \alpha\right) + 0 \tag{11}$$

where α is the alpha operator, i.e., $1\angle 120°$

Equation (10) shows the $I_a - I_b$ connection in terms of symmetrical components. From (11) we see that the zero-sequence currents cancel, and only positive- and negative-sequence currents flow. However, although delta connections effectively eliminate zero-sequence currents, delta connections also create phase shifts.

For wye-delta transformers this phase shift is desirable, but not for autotransformers or wye-wye connected transformers. With autotransformers or wye-wye connected transformers, the HV and LV currents are in phase with each other (or 180° out of phase), and using a delta connection to remove the zero-sequence current will introduce an undesirable 30° phase shift between the HV and LV currents.

Fortunately, numerical relays make it possible to mathematically remove zero-sequence current without creating a phase shift. Perform the following calculation to remove the zero-sequence current from the A-phase current:

$$I_{A\,COMP} = \left(I_A - I_0\right)$$

where $I_0 = \frac{1}{3}\left(I_A + I_B + I_C\right)$

$$I_{A\,COMP} = \left[I_A - \frac{1}{3}\left(I_A + I_B + I_C\right)\right]$$

$$I_{A\,COMP} = \frac{1}{3}\left(3I_A - I_A - I_B - I_C\right)$$

$$I_{A\,COMP} = \frac{1}{3}\left(2I_A - I_B - I_C\right)$$

Similarly for the B- and C-phases:

$$I_{B\,COMP} = \frac{1}{3}\left(2I_B - I_A - I_C\right)$$

$$I_{C\,COMP} = \frac{1}{3}\left(2I_C - I_B - I_A\right)$$

Arranging the results in matrix form yields the following:

$$\begin{bmatrix} I_{A\,COMP} \\ I_{B\,COMP} \\ I_{C\,COMP} \end{bmatrix} = \frac{1}{3} \begin{bmatrix} 2 & -1 & -1 \\ -1 & 2 & -1 \\ -1 & -1 & 2 \end{bmatrix} \bullet \begin{bmatrix} I_A \\ I_B \\ I_C \end{bmatrix}$$

Matrix 0 is the identity matrix, and does not alter the currents.

$$\begin{bmatrix} I_{A\,COMP} \\ I_{B\,COMP} \\ I_{C\,COMP} \end{bmatrix} = \begin{bmatrix} 1 & 0 & 0 \\ 0 & 1 & 0 \\ 0 & 0 & 1 \end{bmatrix} \bullet \begin{bmatrix} I_A \\ I_B \\ I_C \end{bmatrix}$$

VIII. REFERENCES

[1] SEL-387-0, -5, -6 Instruction Manual, date code 20050919.

[2] Blackburn, J. Lewis. *Symmetrical Components for Power System Engineering*, New York: M. Dekker, 1993.

[3] Anderson, Paul M. *Analysis of Faulted Power Systems*. IEEE Press power system engineering series. New York: IEEE Press, 1995.

[4] Harlowe, James H., ed. *Electric Power Transformer Engineering*, Boca Raton, FL: CRC Press, 2004.

IX. BIOGRAPHY

Casper Labuschagne earned his Diploma (1981) and Masters Diploma (1991) in Electrical Engineering from Vaal Triangle Technicon, South Africa. After gaining 20 years of experience with the South African utility Eskom where he served as Senior Advisor in the protection design department, he began work at SEL in 1999 as a Product Engineer in the Substation Equipment Engineering group. In 2003 he transferred to his present position as Lead Engineer in the Research and Development group where his responsibilities include the specification, design, and testing of protection and control devices. Casper is registered as a Professional Technologist with ECSA, the Engineering Counsel of South Africa, and has authored and co-authored several technical papers.

Normann Fischer joined Eskom as a Protection Technician in 1984. He received a Higher Diploma in Technology, with honors, from the Witwatersrand Technikon, Johannesburg, in 1988, a B.Sc. in Electrical Engineering, with honors, from the University of Cape Town in 1993, and an M.S.E.E. from the University of Idaho in 2005. He was a Senior Design Engineer in Eskom's Protection Design Department for three years, then joined IST Energy as a Senior Design Engineer in 1996. In 1999, he joined Schweitzer Engineering Laboratories as a Power Engineer in the Research and Development Division. He was a registered professional engineer in South Africa and a member of the South Africa Institute of Electrical Engineers.

Previously presented at the 2007 Texas A&M Conference for Protective Relay Engineers.

20060915 • TP6259-01